Title

Growth response of temperate mountain grasslands to inter-annual variations of snow cover duration

Running title

Growth response of grasslands to snow cover duration

Author

Philippe Choler[1,2,3] *

Addresses

[1] Univ. Grenoble Alpes, LECA, F-38000 Grenoble, France

[2] CNRS, LECA, F-38000 Grenoble, France

[3] LTER "Zone Atelier Alpes", F-38000 Grenoble, France

Contact detail

* Laboratoire d'Ecologie Alpine, UMR CNRS-UJF 5553, Université Grenoble Alpes, BP53, 38041 Grenoble, France. Tel (33) 4 76 51 45 43. Fax (33) 4 76 51 44 63.

E-mail: philippe.choler@ujf-grenoble.fr

Key words: mountain grasslands - NDVI - path analysis - phenology - snow

ABSTRACT (284 WORDS)

A remote sensing approach is used to examine the direct and indirect effects of snow cover duration and weather conditions on the growth response of mountain grasslands located above the tree line in the French Alps. Time-integrated Normalized Difference Vegetation Index (NDVIint), used as a surrogate for aboveground primary productivity, and snow cover duration were derived from a 13-year long time series of the Moderate Resolution Imaging Spectro-radiometer (MODIS). A regional-scale meteorological forcing that accounted for topographical effects was provided by the SAFRAN–CROCUS–MEPRA model chain. A hierarchical path analysis was developed to analyze the multivariate causal relationships between forcing variables and proxies of primary productivity. Inter-annual variations in primary productivity were primarily governed by year-to-year variations in the length of the snow-free period and to a much lesser extent by temperature and precipitation during the growing season. A prolonged snow cover reduces the number and magnitude of frost events during the initial growth period but this has a negligible impact on NDVIint as compared to the strong negative effect of a delayed snow melting. The maximum NDVI slightly responded to increased summer precipitation and temperature but the impact on productivity was weak. The period spanning from peak standing biomass to the first snowfall accounted for two thirds of NDVIint and this explained the high sensitivity of NDVIint to autumn temperature and autumn rainfall that control the timing of the first snowfall. The ability of mountain plants to maintain green tissues during the whole snow-free period along with the relatively low responsiveness of peak standing biomass to summer meteorological conditions led to the conclusion that the length of the snow-free period is the primary driver of the inter-annual variations in primary productivity of mountain grasslands.

Introduction

Temperate mountain grasslands are seasonally snow-covered ecosystems that have to cope with a limited period of growth (Körner, 1999). The extent to which the length of the snow-free period controls the primary production of mountain grasslands is still debated. On the one hand, snow cover manipulation experiments and time series analyses of ground-based measurements generally showed a decrease in biomass production under shortened growing season length (Wipf and Rixen, 2010; Rammig et al., 2010). On the other hand, several studies pointed to the increasing risk of spring frost damage and summer water shortage following an early snowmelt and the associated detrimental effects on biomass production (Baptist et al., 2010; Ernakovich et al., 2014; Inouye, 2000). In addition, both soil microbial nitrogen immobilization and accumulation of inorganic nitrogen are enhanced under deep and long-lasting snowpacks (Brooks et al., 1998), and plants may benefit from increased flush of nutrients and ameliorated soil water balance following unusually long winters. To better understand the growth response of alpine grasslands to changing snow cover duration it thus seems pivotal (i) to assess the contribution of the different components of the growth response, particularly the duration of the favorable period of growth and the peak standing biomass; (ii) to account for the effect of meteorological forcing variables on both snow cover dynamics and on plant growth, and (iii) to disentangle the direct and indirect effects, i.e. effects mediated by other forcing variables, of snow cover on land surface phenology and primary productivity.

From a phenomenological point of view, annual primary production may be viewed as the outcome of two things namely the time available for biomass production and the amount of biomass produced per unit of time. For seasonally snow-covered ecosystems, this translates into two fundamental questions: to what

74 extent does the length of the snow-free period determine the length of plant activity?
75 and (ii) what are the main drivers controlling the instantaneous primary production
76 rate of grasslands during the snow-free period? A number of studies have provided
77 evidence for the non-independence of these two facets of growth response by noting
78 that the biomass production rate increases when snow melting is delayed and that
79 grasslands are able to partially recover the time lost when the winter was atypically
80 long (Walker et al., 1994; Jonas et al., 2008). However, most of these studies focused
81 on the initial period of growth - i.e. from the onset of greenness to the time of peak
82 standing biomass - and therefore little is known about the overall relationship between
83 the mean production rate and the total length of the snow-free period. Eddy
84 covariance measurements have shown that the amount of carbon fixed from the peak
85 standing biomass to the first snowfall represents a significant contribution to the
86 Gross Primary Productivity (GPP) (e.g. Rossini et al., 2012). Accounting for the full
87 period of plant activity when examining how primary production of grasslands adjusts
88 to inter-annual variations in meteorological conditions seems thus essential.
89 Remote sensing provides invaluable data for tracking ecosystem phenology
90 over broad spatial scale as well as inter-annual variations of phenological stages over
91 extended time periods (Pettorelli et al., 2005). For temperature-limited ecosystems,
92 numerous studies focused on arctic areas have established that the observed decadal
93 trend toward an earlier snowmelt has translated into extended growing season and
94 enhanced greenness (Myneni et al., 1997; Jia et al., 2003). By contrast, the phenology
95 of high elevation grasslands has not received the same degree of attention, partly
96 because there are a number of methodological problems in using remote sensing data
97 in topographically complex terrain, including scale mismatches, geolocation errors,
98 and vegetation heterogeneity (Fontana et al., 2009; Tan et al., 2006). That said, some

99 studies have used moderate resolution imagery to document the contrasting responses
100 of low and high vegetation to the 2003 heat wave in the Alps (Jolly, 2005; Reichstein
101 et al., 2007) or to characterize the land surface phenology of high elevation areas in
102 the Rockies (Dunn and de Beurs, 2011), the Alps (Fontana et al., 2008) or the Tibetan
103 plateau (Li et al., 2007). However, none of these studies has comprehensively
104 examined the direct and indirect effect of meteorological forcing variables and snow
105 cover duration on the different components of annual biomass production in mountain
106 grasslands.
107 In this paper, I used remotely sensed time series of the Normalized Difference
108 Snow index (NDSI) and of the Normalized Difference Vegetation Index (NDVI) to
109 characterize snow cover dynamics and growth response of mountain grasslands.
110 Time-integrated NDVI (NDVIint) and the product of NDVI and Photosynthetically
111 Active Radiation (PAR) were taken as surrogates of aboveground primary
112 productivity, while maximum NDVI (NDVImax) was used as an indicator of growth
113 responsiveness to weather conditions during the summer. My main aim is to decipher
114 the interplay of snow cover dynamics, weather conditions and growth responsiveness
115 affecting NDVIint. Specifically, I addressed three questions: (i) What is the relative
116 contribution of the growing season length and NDVImax in determining the inter-
117 annual variations of primary productivity ? (ii) What are the direct and indirect
118 effects of the snow cover dynamics on productivity ? and (iii) What is the sensitivity
119 of NDVIint to inter-annual variations in temperature and precipitation during the
120 growing season? The study was based on 121 grassland-covered high elevation sites
121 located in the French Alps. Sites were chosen to enable a remote sensing
122 characterization of their land surface phenology using the Moderate Resolution
123 Imaging Spectro-radiometer (MODIS). Meteorological forcing was provided by the

SAFRAN–CROCUS–MEPRA model chain that accounts for topographical effects (Durand et al., 2009c). I implemented a hierarchical path analysis to analyze the multivariate causal relationships between meteorological forcing, snow cover, and NDVI-derived proxies of grassland phenology and primary productivity.

Material and methods

Selection of study sites

The selection of sites across the French Alps was made by combining several georeferenced databases and expert knowledge. My primary source of information was the 100 m-resolution CORINE land cover 2000 database produced by the European Topic Centre on Spatial Information and Analysis (Commission of the European Communities, 1994) that identifies 44 land cover classes based on the visual interpretation of high-resolution satellite images and from which I selected the class 3.2.1 corresponding to 'Natural grasslands'. Natural grasslands located between 2000 m and 2600 m above sea level were extracted using a 50 m-resolution Digital Elevation Model from the Institut Géographique National (IGN). I then calculated the perimeter (P), area (A) and the mean slope of each resulting group of adjacent pixels, hereafter referred as polygons, and kept only those that had an area greater than 20 ha, an index of compactness ($C= 4\pi A/P^2$) greater than 0.1, and a mean slope smaller than 10°. The first two criteria ensured that polygons were large enough and sufficiently round-shaped to include several 250m MODIS contiguous cells and to limit edge effects. The third criterion reduced the uncertainty in reflectance estimates associated with steep slopes and different aspects within the same polygon. Moreover, steep slopes usually exhibit sparser plant cover with low seasonal amplitude of NDVI, which reduces the signal to noise ratio of remote sensing data. Finally, I visually

149 double-checked the land cover of all polygons by using 50 cm-resolution aerial
150 photographs from 2008 or 2009. This last step was required to discard polygons
151 located within ski-resorts and possibly including patches of sown grasslands, and
152 polygons too close to mountain lakes and including swampy vegetation. I also verified
153 that all polygons were located above the treeline.
154
155 *Climate data*
156 Time series of temperature, precipitation and incoming short-wave radiation
157 were estimated by the SAFRAN–CROCUS–MEPRA meteorological model
158 developed by Meteo-France for the French Alps. Details on input data, methodology,
159 and validation of this model are provided in Durand & al. (2009a; 2009b). To
160 summarize, the model combines observed data from a network of weather stations and
161 estimates from numerical weather forecasting models to provide hourly data of
162 atmospheric parameters including air temperature, precipitation and incoming solar
163 radiation. Simulations are performed for twenty-three different massifs of the French
164 Alps (Fig. 1), each of which is subdivided according to the following topographic
165 classes: 300 m elevation bands, seven slope aspect classes (north, flat, east, south-east,
166 south, south-west and west) and two slope classes (20° or 40°). The delineation of
167 massifs was based on both climatological homogeneity, especially precipitation, and
168 physiographic features. To date, SAFRAN is the only operational product that
169 accounts for topographic features in modelling meteorological land surface
170 parameters for the different massifs of the French Alps.
171
172 *MODIS data*

The MOD09A1 and MOD09Q1 surface reflectance products corresponding to tile h18.v4 (40◦N-50◦N, 0◦E-15.6◦E) were downloaded from the Land Processes Distributed Active Archive Center (LP DAAC) (ftp://e4ftl01.cr.usgs.gov). A total of 499 scenes covering the period from 18-02-2000 to 27-12-2012 were acquired for further processing. Data are composite reflectance, i.e. representing the highest observed value over an 8-day period. Surface reflectance in the red (RED), green (GREEN), near-infrared (NIR) and mid-infrared (MIR) were used to calculate a Normalized Difference Vegetation Index (NDVI) at 250 m following:

$$NDVI = (NIR - RED) / (NIR + RED) \quad \text{(eqn. 1)}$$

and a Normalized Difference Snow Index (NDSI) at 500 m using the algorithm implemented in Salomonson and Appel (2004):

$$NDSI = (GREEN - MIR) / (GREEN + MIR) \quad \text{(eqn. 2)}$$

NDVI and NDSI values were averaged for each polygon. Missing or low quality data were identified by examining quality assurance information contained in MOD09Q1 products and interpolated using cubic smoothing spline. NDVI or NDSI values that were two times larger or smaller than the average of the two preceding values and the two following values were considered as outliers and discarded. Time series were gap-filled using cubic spline interpolation and smoothed using the Savitzky-Golay filter with a moving window of length n = 2 and a quadratic polynomial fitted to 2n + 1 points (Savitzky and Golay, 1964).

A high NDSI and low NDVI were indicative of wintertime whereas a low NDSI and a high NDVI were indicative of the growing season (Fig. 2). Here I used the criteria NDSI / NDVI < 1 to estimate the length of the snow-free period, hereafter referred as Psf, at the polygon level (Fig. 2). This ratio was chosen as a simple and consistent way to set the start (TSNOWmelt) and the end (TSNOWfall) of the snow-

free period across polygons and years. Ground-based observations corresponding to one MOD09A1 pixel (Lautaret pass, 6.4170° longitude and 45.0402° latitude) and including visual inspection, analysis of images acquired with time-lapse cameras and continuous monitoring of soil temperature and snow height showed that this ratio provides a fair estimate of snowcover dynamics (Fig. S1). Further analyses also indicated that Psf is relatively insensitive to changes in the NDVI/NDSI thresholds with 95% of the polygon x year combinations exhibiting less than 2 days of shortening when the threshold was set to 1.1 and less than 3 days of lengthening when the threshold was set to 0.9 (Fig. S2). Finally, changing the threshold within this range had no impact on the main results of the path analysis. The yearly maximum NDVI value (NDVImax) was calculated as the average of the three highest daily consecutive values of NDVI and the corresponding middle date was noted TNDVImax.

The Gross Primary Productivity (GPP) of grasslands could be derived from remote sensing data following a framework originally published by Monteith (Monteith, 1977). In this approach, GPP is modelled as the product of the incident Photosynthetically Active Radiation (PAR), the fraction of PAR absorbed by vegetation (fPAR) and a light-use efficiency parameter (LUE) that expresses the efficiency of light conversion to carbon fixation. It has been shown that fPAR can linearly related to vegetation indices under a large combination of vegetation, soil– and atmospheric conditions (Myneni and Williams, 1994). Assuming that LUE was constant for a given polygon, I therefore approximated inter-annual variations of GPP using the time-integrated value of the product NDVI x PAR, hereafter referred as GPPint, over the growing season and calculated as follows:

$$\text{GPPint} \sim \sum_{t=1}^{T} \text{NDVI}_t \times \text{PAR}_t \qquad \text{(eqn. 3)}$$

where T is the number of days for which NDVI was above NDVIthr. I set NDVIthr = 0.1 having observed lower NDVI usually corresponded to partially snow-covered sites and or to senescent canopies (Fig. 2). The main findings of this study did not change when I varied NDVIthr in the range 0.05-0.15. As a simpler alternative to GPPint, i.e. not accounting for incoming solar radiation, I also calculated the time-integrated value of NDVI, hereafter referred as NDVIint following:

$$\text{NDVIint} = \sum_{t=1}^{T} \text{NDVI}_t \qquad \text{(eqn. 4)}$$

The periods from the beginning of the snow-free period to TNDVImax, hereafter referred as Pg, and from TNDVImax to the end of the first snowfall, hereafter referred as Ps, were used to decompose productivity into two components: NDVIintg and GPPintg, and NVIints and GPPints (Fig. 2). Note that the suffix letters g and s are used to refer to the first and the second part of the growing season, respectively.

The whole analysis was also conducted with the Enhanced Vegetation Index (Huete et al., 2002) instead of NDVI. The rationale for this alternative was to select a vegetation index which was more related to the green biomass and thus may better approximate GPP especially during the senescence period. I did not find any significant change in the main results when using EVI. In particular, the period spanning from peak standing biomass to the first snowfall accounted for two thirds of EVIint as is the case for NDVIint (Fig. S3A) and inter-annual variations in EVIint were of the same order of magnitude as those for NDVIint (Fig. S3B). Because results from the path analysis (see below) were also very similar with EVI-based proxies of productivity, I chose to present NDVI-based results only.

Path analysis

247 Path analysis represents an appropriate statistical framework to model
248 multivariate causal relationships among observed variables (Grace et al., 2010). Here,
249 I examined different causal hypotheses of the cascading effects of meteorological
250 forcing, snow cover duration and phenological parameters (TNDVImax, Pg, and Ps)
251 on NDVIint and GPPint. To better contrast the processes involved during different
252 stages of the growing season, separate models were implemented for the period of
253 growth and the period of senescence. The set of causal assumptions is represented
254 using directed acyclic graphs in which arrows indicate which variables are influencing
255 (and are influenced by) other variables. These graphs may include both direct and
256 indirect effects. An indirect effect of X1 on Y means that the effect of X1 is mediated
257 by another variable (for example X1->X2->Y). Path analysis tests the degree to which
258 patterns of variance and covariance in the data are consistent with hypothesized causal
259 links. To develop this analysis, three main assumptions have been made: (i) that the
260 graphs do not include feedbacks (for example, X1->X2->Y->X2); (ii) that the
261 relationships among variables can be described by linear models and (iii) that annual
262 observations are independent, i.e. the growth response in year n is not influenced by
263 previous years because of carryover effects.
264 Since I chose to focus on the inter-annual variability of growth response, I
265 removed between-site variability by calculating standardized anomalies for each
266 polygon. Standardized anomalies were calculated by dividing annual anomalies by
267 the standard deviation of the time series making the magnitude of the anomalies
268 comparable among sites.
269 For each causal diagram, partial regression coefficients were estimated for the
270 whole dataset and for each polygon. These coefficients measure the extent of an effect
271 of one variable on another while controlling for other variables. Model estimates were

272 based on maximum likelihood, and Akaike Information Criterion (AIC) was used to
273 compare performance among competing models. Only ecologically meaningful
274 relationships were tested. The model with the lowest AIC was retained as being the
275 most consistent with observed data.
276 I used the R software environment (R Development Core Team, 2010) to
277 perform all statistical analyses. Path coefficients and model fit were estimated using
278 the package *lavaan* (Rosseel, 2012).

Results

One hundred and twenty polygons fulfilling the selection criteria were included in the analyses. These polygons spanned 2° of latitude and more than 1° of longitude and were distributed across seventeen massifs of the French Alps from the Northern part of Mercantour to the Mont-Blanc massif (Fig. 1). Their mean elevation ranged from 1998 m to 2592 m with a median of 2250 m. Noticeably, many polygons were located in the Southern and in the innermost part of the French Alps where high elevation landscapes with grassland-covered gentle slopes are more frequent essentially because of the occurrence of flysch, a bedrock on which deep soil formation is facilitated.

A typical yearly course of NDVI and NDSI is shown in Figure 2. The date at which the NDSI/NDVI ratio crosses the threshold of one was very close to the date at which NDVI crosses the threshold of 0.1. On average, NDVImax was reached fifty days after snowmelt, a period corresponding to only one third of the length of the snow-free period (Fig. 3A). Similarly, NDVIg accounted for one third of the NDVIint (Fig. 3B). The contribution of the first part of season was slightly higher for GPPint though it largely remained under 50% (Fig. 3C). Thus, the maintained vegetation greenness from TNDVImax to TSNOWfall explained the dominant contribution of the second part of the growing season to NDVI-derived proxies of grassland productivity.

Most of the variance in NDVIint and GPPint was accounted for by between-polygon variations that were higher during the period of senescence compared to the period of growth (Table 1). Inter-annual variations of NDVIint and GPPint represented 25% of the total variance and were particularly pronounced at the end of the examined period with the best year (2011) sandwiched by two (2010, 2012) of the

three worst years (Fig. 4A). The two likely proximal causes of these inter-annual variations, i.e. Psf and NDVImax, showed highly contrasted variance partitioning. Between-year variation in Psf was four to five times higher than that of NDVImax (Table 1). The standardized inter-annual anomalies of Psf showed remarkable similarities with those of NDVIint and GPPint both in terms of magnitude and direction (Fig. 4B). By contrast, the small inter-annual variations of NDVImax did not relate to inter-annual variations of NDVIint or GPPint (Fig. 4C). For example, the year 2010 had the strongest negative anomaly for both Psf and NDVIint whereas the NDVImax anomaly was positive. There were some discrepancies between the two proxies of primary productivity. For example, the heat wave of 2003, which yielded the highest NDVImax, exhibited a much stronger positive anomaly for GPPint than for NDVIint and this was due to the unusually high frequency of clear sky during this particular summer.

The path analysis confirmed that the positive effect of the length of the period available for plant activity largely surpassed that of NDVImax to explain inter-annual variations of NDVIint and GPPint. This held true for NDVIintg or GPPintg - with an over dominating effect of Pg (Fig. 5A, C) - and for NDVIints or GPPints - with an over dominating effect of Ps (Fig. 5B, D). There was some support for an indirect effect of Pg on productivity mediated by NDVImax, as removing the path Pg-> NDVImax in the model decreased its performance (Table 2). In addition to shortening the time available for growth and reducing primary productivity, a delayed snowmelt also significantly decreased the number of frost events and this had a weak positive effect on both NDVIintg and GPPintg (Fig. 5A, C). However, this positive and indirect effect of TSNOWmelt on productivity, which amounts to (-0.46) x (-0.08) = 0.04 for NDVIintg and (-0.46) x (-0.13) = 0.06 for GPPintg, was small compared to

329 the negative effect of TSNOWmelt on NDVIintg (-1 x 0.96 for NDVIintg and -1 x
330 0.95 for GPPintg). Apart from its effect on frost events and Ps, TSNOWmelt had also
331 a significant positive effect on TNDVImax with a path coefficient of 0.57, signifying
332 that grasslands partially recover the time lost because of a long winter to reach peak
333 standing biomass. On average, a one-day delay in the snowmelt date translates to a
334 0.5-day delay in TNDVImax (Fig. S4A).

335 Compared to snow-cover dynamics, weather conditions during the growing
336 period had relatively small effects on both NDVImax and productivity (Fig. 5). For
337 example, removing the effects of temperature on NDVImax and precipitation on
338 NDVIintg did not change model fit (Table 2). The most significant positive effects of
339 weather conditions were observed during the senescence period and more specifically
340 for GPPints with a strong positive effect of temperature (Fig. 5D). The impact of
341 warm and dry days on incoming radiation explained why more pronounced effects of
342 temperature and precipitation are observed for GPPint (Fig. 5D), which is dependent
343 upon PAR (see eqn. 3), than for NDVIint (Fig. 5B).

344 Meteorological variables governing snow cover dynamics had a strong impact
345 on primary productivity (Fig. 5). A warm spring advancing snowmelt translated into a
346 significant positive effect on NDVIintg and GPPintg - an indirect effect which
347 amounts to (-0.62) x (-1) x 0.95 =0.59 (Fig. 5A, C). Heavy precipitation and low
348 temperature in October-November caused early snowfall and shortened Ps, which
349 severely reduced NDVIints and GPPints (Fig. 5B, D). Overall, given that the
350 senescence period accounted for two thirds of the annual productivity (Fig. 3B, C),
351 the determinants of the first snowfall were of paramount importance for explaining
352 inter-annual variations of NDVIint and GPPint.

353 Path coefficients estimated for each polygon showed that the magnitude and
354 direction of the direct and indirect effects were highly conserved across the polygons.
355 The climatology of each polygon was estimated by averaging growing season
356 temperature and precipitation across the 13 years. Whatever the path coefficient,
357 neither of these two variables explained more than 8% of variance of the between-
358 polygon variation (Table 3). The two observed trends were (i) a greater positive effect
359 of NDVImax on NDVIintg in polygons receiving more rainfall, which was consistent
360 with the significant effect of precipitation on NDVImax (Fig. 5A) and (ii) a smaller
361 effect of temperature and Ps on GPPints and NDVIints, respectively, suggesting that
362 the coldest polygons were less responsive to increased temperatures or lengthening of
363 the growing period (see discussion).
364

Discussion

Using a remote sensing approach, I showed that inter-annual variability in NDVI-derived proxies of productivity in alpine grasslands was primarily governed by variations in the length of the snow-free period. As a consequence, meteorological variables controlling snow cover dynamics are of paramount importance to understand how grassland growth adjusts to changing conditions. This was especially true for the determinants of the first snowfall, given that the period spanning from the peak standing biomass onwards accounted for two-thirds of annual grassland productivity. By contrast, NDVImax - taken as an indicator of growth responsiveness - showed small inter-annual variation and weak sensitivity to summer temperature and precipitation. Overall, these results highlighted the ability of grasslands to track inter-annual variability in the timing of the favorable season by maintaining green tissues during the whole snow-free period and their relative inability to modify the magnitude of the growth response to the prevailing meteorological conditions during the summer. I discuss below these main findings in light of our current understanding of extrinsic and intrinsic factors controlling alpine grassland phenology and growth.

In spring, the sharp decrease of NDSI and the initial increase of NDVI were simultaneous events (Fig. 2). Previous reports have shown that NDVI may increase independently of greenness during the snow melting period (Dye and Tucker, 2003) and this has led to the search for vegetation indices other than NDVI to precisely estimate the onset of greenness in snow-covered ecosystems (Delbart et al., 2006). Here I did not consider that the period of plant activity started with the initial increase of NDVI. Instead I combined NDVI and NDSI indices to estimate the date of snowmelt and then used a threshold value of NDVI = 0.1 before integrating NDVI over time. By doing this, I strongly reduced the confounding effect of snowmelt on

390 the estimate of the onset of greenness. That said, a remote sensing phenology may fail
391 to accurately capture the onset of greenness for many other reasons, including
392 smoothing procedures applied to NDVI time series, inadequate thresholds,
393 geolocation uncertainties, mountain terrain complexity and vegetation heterogeneity
394 (Cleland et al., 2007; Tan et al., 2006; Dunn and de Beurs, 2011; Doktor et al., 2009).
395 Assessing the magnitude of this error is difficult as there have been very few studies
396 comparing ground-based phenological measurements with remote sensing data, and
397 furthermore most of the available studies have focused on deciduous forests
398 (Hmimina et al., 2013; Busetto et al., 2010; but see Fontana et al., 2008). Ground-
399 based observations collected at one high elevation site and corresponding to a single
400 MOD09A1 pixel provide preliminary evidence that the NDVI/NDSI criterion
401 adequately captures snowcover dynamics (Fig. S3). Further studies are needed to
402 evaluate the performance of this metric at a regional scale. For example, the analysis
403 of high-resolution remote sensing data with sufficient temporal coverage is a promising way
404 to monitor snow cover dynamics in complex alpine terrain and to assess its impact on the
405 growth of alpine grasslands (Carlson et al., 2015). Such an analysis has yet to be done at a
406 regional scale. Despite these limitations, I am confident that the MODIS-derived
407 phenology is appropriate for addressing inter-annual variations of NDVIint because:
408 (i) the start of the season shows low NDVI values and thus uncertainty in the green-up
409 date will marginally affect integrated values of NDVI and GPP, and (ii) beyond errors
410 in estimating absolute dates, remote sensing has been shown to adequately capture the
411 inter-annual patterns of phenology for a given area (Fisher and Mustard, 2007; Studer
412 et al., 2007), and this is precisely what is undertaken here.

413 Regardless of the length of the winter, there was no significant time lag
414 between snow disappearance and leaf greening at the polygon level. This is in

agreement with many field observations showing that initial growth of mountain plants is tightly coupled to snowmelt timing (Körner, 1999). This plasticity in the timing of the initial growth response, which is enabled by tissue preformation, is interpreted as an adaptation to cope with the limited period of growth in seasonally snow-covered ecosystems (Galen and Stanton, 1991). Early disappearance of snow is controlled by spring temperature, and our results showing that a warm spring leads to a prolonged period of plant activity are consistent with those originally reported from high latitudes (Myneni et al., 1997). Other studies have also shown that the onset of greenness in the Alps corresponds closely with year-to-year variations in the date of snowmelt (Stockli and Vidale, 2004) and that spring mean temperature is a good predictor of melt out (Rammig et al., 2010). This study improves upon previous works (i) by carefully selecting targeted areas to avoid mixing different vegetation types when examining growth response, (ii) by using a meteorological forcing that is more appropriate to capture topographical and regional effects compared to global meteorological gridded data (Frei and Schär, 1998), and (iii) by implementing a statistical approach enabling the identification of direct and indirect effects of snow on productivity.

Even if there were large between-year differences in Pg, the magnitude of year-to-year variations in NDVImax were small compared to that of NDVIint or GPPint (Table 1 and Fig. 4). Indeed, initial growth rates buffer the impact of inter-annual variations in snowmelt dates, as has already been observed in a long-term study monitoring seventeen alpine sites in Switzerland (Jonas et al., 2008). Essentially, the two contrasting scenarios for the initial period of growth observed in this study were either a fast growth rate during a shortened growing period in the case of a delayed snowmelt, or a lower growth rate over a prolonged period following a

warm spring. These two dynamics resulted in nearly similar values of NDVImax as TSNOWmelt explained only 4% of the variance in NDVImax (Fig. S4B). I do not think that the low variability in the response of NDVImax to forcing variables is due to a limitation of the remote sensing approach. First, there was a high between-site variability of NDVImax, indicating that the retrieved values were able to capture variability in the peak standing aboveground biomass (Table 1). Second, the mean NDVImax of the targeted areas is around 0.7 (Fig. 4B), i.e. in a range of values where NDVI continues to respond linearly to increasing green biomass and Leaf Area Index (Hmimina et al., 2013). Indeed, many studies have shown that the maximum amount of biomass produced by arctic and alpine species or meadows did not benefit from the experimental lengthening of the favorable period of growth (Kudo et al., 1999; Baptist et al., 2010), or to increasing CO2 concentrations (Körner et al., 1997). Altogether, these results strongly suggest that intrinsic growth constraints limit the ability of high elevation grasslands to enhance their growth under ameliorated atmospheric conditions. More detailed studies will help us understanding the phenological response of different plant life forms (e.g. forbs and graminoids) to early and late snowmelting years and their contribution to ecosystem phenology (Julitta et al., 2014). Other severely limiting factors - including nutrient availability in the soil - may explain this low responsiveness (Körner, 1989). For example, Vittoz & al. (2009) emphasized that year-to-year changes in the productivity of mountain grasslands were primarily caused by disturbance and land use changes that affect nutrient cycling. Alternatively, one cannot rule out the possibility that other bioclimatic variables could better explain the observed variance in NDVImax. For example, the inter-annual variations in precipitation had a slight though significant effect on NDVImax (Fig.

5A, C) suggesting that including a soil water balance model might improve our understanding of growth responsiveness, as suggested by (Berdanier and Klein, 2011). Many observations and experimental studies have also pointed out that soil temperature impacts the distribution of plant and soil microbial communities (Zinger et al., 2009), ecosystem functioning (Baptist and Choler, 2008), and flowering phenology (Dunne et al., 2003). More specifically, the lack of snow or the presence of a shallow snowpack during winter increase the frequency of freezing and thawing events with consequences on soil nutrient cycling and aboveground productivity (Kreyling et al., 2008; Freppaz et al., 2007). Thus, an improvement of this study would be to test, not only for the effect of presence-absence of snow, but also for the effect of snowpack height and soil temperature on NDVImax and growth responses of alpine pastures. Regional climate downscaling of soil temperature at different depths is currently under development within the SAFRAN-CROCUS-MEPRA model chain and there will be future opportunities to examine these linkages. Nevertheless, the results showed that at the first order the summer meteorological forcing was instrumental in controlling GPPints, without having a direct effect on NDVImax (Fig.5B, D). In particular, positive temperature anomalies and associated clear skies had significant effects on GPPints. Moreover, path analysis conducted at the polygon level also provided some evidence that responsiveness to ameliorated weather conditions was less pronounced in the coldest polygons (Table 3), suggesting stronger intrinsic growth constraints in the harshest conditions. Collectively, these results indicated that the mechanism by which increased summer temperature may enhance grassland productivity was through the persistence of green tissues over the whole season rather than through increasing peak standing biomass.

The contribution of the second part of the summer to annual productivity has been overlooked in many studies (e.g. Walker et al., 1994; Rammig et al., 2010; Jonas et al., 2008; Jolly et al., 2005) that have primarily focused on early growth, or on the

490 amount of aboveground biomass at peak productivity. Here, I showed that the length
491 of the senescing phase is a major determinant of inter-annual variation in growing
492 season length and productivity and hence that temperature and precipitation in
493 October-November are strong drivers of these inter-annual changes (Fig. 5B, D). The
494 importance of autumn phenology was recently re-evaluated in remote sensing studies
495 conducted at global scales (Jeong et al., 2011; Garonna et al., 2014). A significant
496 long-term trend towards a delayed end of the growing season was noticed for Europe
497 and specifically for the Alps. In the European Alps, temperature and moisture regimes
498 in late autumn and early winter are possibly under the influence of the North Atlantic
499 Oscillation (NAO) phase anomalies (Beniston and Jungo, 2002). This opens the way
500 for research on teleconnections between oceanic and atmospheric conditions and the
501 regional drivers of alpine grassland phenology and growth.
502 Eddy covariance data also provided direct evidence that the second half of the
503 growing season is a significant contributor to the annual GPP of mountain grasslands
504 (Chen et al., 2009; Rossini et al., 2012; Li et al., 2007; Kato et al., 2006). However it
505 has also been shown that while the combination of NDVI and PAR successfully
506 captured daily GPP dynamics in the first part of the season, NDVI tended to provide
507 an overestimate of GPP in the second part (Chen et al., 2009; Li et al., 2007). Possible
508 causes include decreasing light-use efficiency in the end of the growing season in
509 relation to the accumulation of senescent material and/or the "dilution" of leaf
510 nitrogen content by fixed carbon. Noticeably, the main findings of this study did not
511 change when NDVI was replaced by EVI, a vegetation index which is more sensitive
512 to green biomass and thus may better capture primary productivity. Consistent with
513 this result, Rossini et al. (2012) did not find any evidence that EVI-based proxies
514 performed better than NDVI-based proxies to estimate the GPP of a subalpine pasture.

Further comparison with other vegetation indexes - like the MTCI derived from MERIS products (Harris and Dash, 2010) – will contribute to better evaluate NDVI-based proxies of GPP.

A strong assumption of this study was to consider that the LUE parameter is constant across space and time. There is still a vivid debate on the relevance of using vegetation specific LUE in remote sensing studies of productivity (Yuan et al., 2014; Chen et al., 2009). Following Yuan & al. (2014) I have assumed that variations in light-use efficiency are primarily captured by variations in NDVI because this vegetation index correlates with structural and physiological properties of canopies (e.g. leaf area index, chlorophyll and nitrogen content). Multiple sources of uncertainty affect remotely sensed estimates of productivity and it is questionnable whether the product NDVI times PAR is a robust predictor of GPP in alpine pastures. The estimate of absolute values of GPP and its comparison across sites was not the aim of this study that focuses on year-to-year relative changes of productivity for a given site. It is assumed that limitations of a light-use efficiency model are consistent across time and that these limitations did not prevent the analysis of the multiple drivers affecting inter-annual variations of remotely sensed proxies of GPP. At present, there is no alternative for regional-scale assessment of productivity using remote sensing data. In the future, possible improvements could be made by using air-borne hyperspectral data to derive spatial and temporal changes in the functional properties of canopies (Ustin et al., 2004) and assess their impact on annual primary productivity.

Conclusions

I have shown that the length of the snow-free period is the primary determinant of remote sensing-based proxies of primary productivity in temperate mountain grasslands. From a methodological point of view, this study demonstrated the relevance of path analysis as a means to decipher the cascading effects and relative contributions of multiple predictors on grassland phenology and growth. Overall, these findings call for a better linkage between phenomenological models of mountain grassland phenology and growth and land surface models of snow dynamics. They open the way to a process-based, biophysical modelling of alpine pastures growth in response to environmental forcing following an approach used in a different climate (Choler et al., 2010). Year-to-year variability in snow cover in the Alps is high (Beniston et al., 2003) and climate-driven changes in snow cover are on-going (Hantel et al., 2000; Keller et al., 2005; Beniston et al., 1997). Understanding the factors controlling the timing and amount of biomass produced in mountain pastures thus represents a major challenge for agro-pastoral economies.

Acknowledgements

This research was conducted on the long-term research site Zone Atelier Alpes, a member of the ILTER-Europe network. This work has been partly supported by a grant from Labex OSUG@2020 (Investissements d'avenir – ANR10 LABX56) and from the Zone Atelier Alpes. The author is part of Labex OSUG@2020 (ANR10 LABX56). Two anonymous reviewers provided constructive comments on the first version of this manuscript. Thanks are due to Yves Durand for providing SAFRAN-CROCUS regional climate data, to Jean-Paul Laurent for the monitoring of snow cover dynamics at the Lautaret pass and to Brad Carlson for his helpful comments on an earlier version of this manuscript.

565 **Table 1**

566 Variance partitioning into between-polygon and between-year components for the set

567 of predictors and growth responses included in the path analysis.

568

		Percentage of variance	
Variable	Abbreviation	between polygons	between years
Date of snow melting	TSNOWmelt	53.6	46.4
Date of first snowfall	TSNOWfall	15.7	84.3
Length of the snow-free period	Psf	48.2	51.8
Length of the period of growth	Pg	27.9	72.1
Length of the period of senescence	Ps	40.5	59.5
Date of NDVImax	TNDVImax	41.4	58.6
Maximum NDVI	NDVImax	87.9	12.1
Time-integrated NDVI over Psf	NDVIint	73.3	26.7
Time-integrated NDVI over Pg	NDVIintg	37.6	62.4
Time-integrated NDVI over Ps	NDVIints	61.3	38.7
Time-integrated NDVIxPAR over Psf	GPPint	73.4	26.6
Time-integrated NDVIxPAR over Pg	GPPintg	32.5	67.5
Time-integrated NDVIxPAR over Ps	GPPints	53.9	46.1

569

570

571 **Table 2**

572 Model fit of competing path models. AIC is the Akaike Information Criteria value and

573 ΔAIC is the difference in AIC between the best model and alternative models.

574

Model	Path diagram	d.f.	AIC	ΔAIC
NDVIintg	as in Fig. 5A	21	28539	0
	removing TEMPg -> NDVImax	22	28540	1
	removing PRECg -> NDVIintg	22	28538	-1
	removing FrEv -> NDVIintg	21	28588	49
	removing Pg -> NDVImax	22	28631	91
NDVIints	as in Fig. 5B	19	30378	82
	removing TNDVImax -> NDVImax	15	30296	0
GPPintg	as in Fig. 5C	21	29895	0
	removing TEMPg -> NDVImax	22	29896	1
	removing PRECg -> GPPintg	22	29924	29
	removing FrEv -> GPPintg	21	29965	70
	removing Pg -> NDVImax	22	29987	92
GPPints	as in Fig. 5D	19	31714	34
	removing TNDVImax -> NDVImax	15	31680	0

575

576

577 **Table 3**

578 Relationships between mean temperature or precipitation of polygons and the path

579 coefficients estimated at the polygon level. Only significant relationships are shown.

580 * P<0.05; ** P<0.01; *** P<0.001.

581

Path	Explanatory variable	Direction of effect	R^2 and significance
PRECg -> GPPintg	Temperature	-	0.04
TGspring -> TSNOWmelt	Precipitation	-	0.05*
NDVImax -> NDVIintg	Precipitation	+	0.07***
TEMPs -> NDVIints	Temperature	-	0.04*
TEMPs -> GPPints	Temperature	-	0.07***
PRECs -> NDVIints	Temperature	+	0.05*
NDVImax -> NDVIints	Temperature	+	0.03*
NDVImax -> GPPints	Temperature	+	0.04*
Ps -> NDVIints	Temperature	-	0.08***
Ps -> NDVIints	Precipitation	+	0.02*

582

583

584 **References**

585 Baptist, F., and Choler, P.: A simulation of the importance of length of growing
586 season and canopy functional properties on the seasonal gross primary production of
587 temperate alpine meadows, Ann. Bot., 101, 549-559, 10.1093/aob/mcm318, 2008.
588 Baptist, F., Flahaut, C., Streb, P., and Choler, P.: No increase in alpine snowbed
589 productivity in response to experimental lengthening of the growing season, Plant
590 Biol., 12, 755-764, 10.1111/j.1438-8677.2009.00286.x, 2010.
591 Beniston, M., Diaz-Henry-F, e., Beniston-Martin, e., and Bradley-Raymond-S, e.:
592 Variations of snow depth and duration in the Swiss Alps over the last 50 years :
593 Links to changes in large-scale climatic forcings. Climatic change at high elevation
594 sites, Clim. Change, 36, 281-300, 1997.
595 Beniston, M., and Jungo, P.: Shifts in the distributions of pressure, temperature and
596 moisture and changes in the typical weather patterns in the Alpine region in response
597 to the behavior of the North Atlantic Oscillation, Theoretical and Applied
598 Climatology, 71, 29-42, 2002.
599 Beniston, M., Keller, F., and Goyette, S.: Snow pack in the Swiss Alps under
600 changing climatic conditions: an empirical approach for climate impacts studies,
601 Theoretical and Applied Climatology, 74, 19-31, 2003.
602 Berdanier, A. B., and Klein, J. A.: Growing Season Length and Soil Moisture
603 Interactively Constrain High Elevation Aboveground Net Primary Production,
604 Ecosystems, 14, 963-974, 10.1007/s10021-011-9459-1, 2011.
605 Brooks, P. D., Williams, M. W., and Schmidt, S. K.: Inorganic nitrogen and microbial
606 biomass dynamics before and during spring snowmelt, Biogeochemistry, 43, 1-15;
607 12, 1998.

608 Busetto, L., Colombo, R., Migliavacca, M., Cremonese, E., Meroni, M., Galvagno,
609 M., Rossini, M., Siniscalco, C., Morra Di Cella, U., and Pari, E.: Remote sensing of
610 larch phenological cycle and analysis of relationships with climate in the Alpine
611 region, Global Change Biol., 10.1111/j.1365-2486.2010.02189.x, 2010.
612 Carlson, B. Z., Choler, P., Renaud, J., Dedieu, J.-P., and Thuiller, W.: Modelling
613 snow cover duration improves predictions of functional and taxonomic diversity for
614 alpine plant communities, Ann. Bot., 10.1093/aob/mcv041, 2015.
615 Chen, J., Shen, M. G., and Kato, T.: Diurnal and seasonal variations in light-use
616 efficiency in an alpine meadow ecosystem: causes and implications for remote
617 sensing, Journal of Plant Ecology, 2, 173-185, 10.1093/jpe/rtp020, 2009.
618 Choler, P., Sea, W., Briggs, P., Raupach, M., and Leuning, R.: A simple
619 ecohydrological model captures essentials of seasonal leaf dynamics in semi-arid
620 tropical grasslands, Biogeosciences, 7, 907-920, 10.5194/bg-7-907-2010, 2010.
621 Cleland, E. E., Chuine, I., Menzel, A., Mooney, H. A., and Schwartz, M. D.: Shifting
622 plant phenology in response to global change, Trends Ecol. Evol., 22, 357-365,
623 2007.
624 Commission of the European Communities: CORINE Land Cover. Technical Guide.
625 Office for Official Publications of European Communities, Luxembourg., 1994.
626 Delbart, N., Letoan, T., Kergoat, L., and Fedotova, V.: Remote sensing of spring
627 phenology in boreal regions: A free of snow-effect method using NOAA-AVHRR
628 and SPOT-VGT data (1982–2004), Remote Sens. Environ., 101, 52-62,
629 10.1016/j.rse.2005.11.012, 2006.
630 Doktor, D., Bondeau, A., Koslowski, D., and Badeck, F. W.: Influence of
631 heterogeneous landscapes on computed green-up dates based on daily AVHRR

632 NDVI observations, Remote Sens. Environ., 113, 2618-2632,
633 10.1016/j.rse.2009.07.020, 2009.
634 Dunn, A. H., and de Beurs, K. M.: Land surface phenology of North American
635 mountain environments using moderate resolution imaging spectroradiometer data,
636 Remote Sens. Environ., 115, 1220-1233, 10.1016/j.rse.2011.01.005, 2011.
637 Dunne, J. A., Harte, J., and Taylor, K. J.: Subalpine meadow flowering phenology
638 responses to climate change: Integrating experimental and gradient methods, Ecol.
639 Monogr., 73, 69-86, 10.1890/0012-9615(2003)073[0069:smfprt]2.0.co;2, 2003.
640 Durand, Y., Giraud, G., Laternser, M., Etchevers, P., Merindol, L., and Lesaffre, B.:
641 Reanalysis of 47 Years of Climate in the French Alps (1958-2005): Climatology and
642 Trends for Snow Cover, Journal of Applied Meteorology and Climatology, 48,
643 2487-2512, 10.1175/2009jamc1810.1, 2009a.
644 Durand, Y., Laternser, M., Giraud, G., Etchevers, P., Lesaffre, B., and Merindol, L.:
645 Reanalysis of 44 Yr of Climate in the French Alps (1958-2002): Methodology,
646 Model Validation, Climatology, and Trends for Air Temperature and Precipitation,
647 Journal of Applied Meteorology and Climatology, 48, 429-449,
648 10.1175/2008jamc1808.1, 2009b.
649 Durand, Y., Laternser, M., Giraud, G., Etchevers, P., Lesaffre, B., and Mérindol, L.:
650 Reanalysis of 44 Yr of Climate in the French Alps (1958–2002): Methodology,
651 Model Validation, Climatology, and Trends for Air Temperature and Precipitation,
652 Journal of Applied Meteorology and Climatology, 48, 429-449,
653 10.1175/2008jamc1808.1, 2009c.
654 Dye, D. G., and Tucker, C. J.: Seasonality and trends of snow-cover, vegetation index,
655 and temperature in northern Eurasia, Geophys. Res. Lett., 30, 9-12, 2003.

656 Ernakovich, J. G., Hopping, K. A., Berdanier, A. B., Simpson, R. T., Kachergis, E. J.,
657 Steltzer, H., and Wallenstein, M. D.: Predicted responses of arctic and alpine
658 ecosystems to altered seasonality under climate change, Glob Chang Biol, 20, 3256-
659 3269, 10.1111/gcb.12568, 2014.
660 Fisher, J. I., and Mustard, J. F.: Cross-scalar satellite phenology from ground,
661 Landsat, and MODIS data, Remote Sens. Environ., 109, 261-273, 2007.
662 Fontana, F., Rixen, C., Jonas, T., Aberegg, G., and Wunderle, S.: Alpine grassland
663 phenology as seen in AVHRR, VEGETATION, and MODIS NDVI time series - a
664 comparison with in situ measurements, Sensors, 8, 2833-2853, 2008.
665 Fontana, F. M. A., Trishchenko, A. P., Khlopenkov, K. V., Luo, Y., and Wunderle, S.:
666 Impact of orthorectification and spatial sampling on maximum NDVI composite
667 data in mountain regions, Remote Sens. Environ., 113, 2701-2712,
668 10.1016/j.rse.2009.08.008, 2009.
669 Frei, C., and Schär, C.: A precipitation climatology of the Alps from high-resolution
670 rain-gauge observations, International Journal of Climatology, 18, 873-900, 1998.
671 Freppaz, M., Williams, B. L., Edwards, A. C., Scalenghe, R., and Zanini, E.:
672 Simulating soil freeze/thaw cycles typical of winter alpine conditions: Implications
673 for N and P availability, Appl. Soil Ecol., 35, 247-255, 2007.
674 Galen, C., and Stanton, M. L.: Consequences of emergent phenology for reproductive
675 success in *Ranunculus adoneus* (Ranunculaceae), Am. J. Bot., 78, 447-459, 1991.
676 Garonna, I., De Jong, R., De Wit, A. J. W., Mucher, C. A., Schmid, B., and
677 Schaepman, M. E.: Strong contribution of autumn phenology to changes in satellite-
678 derived growing season length estimates across Europe (1982-2011), Global Change
679 Biol., 20, 3457-3470, 10.1111/gcb.12625, 2014.

680 Grace, J. B., Anderson, T. M., Olff, H., and Scheiner, S. M.: On the specification of
681 structural equation models for ecological systems, Ecol. Monogr., 80, 67-87,
682 10.1890/09-0464.1, 2010.
683 Hantel, M., Ehrendorfer, M., and Haslinger, A.: Climate sensitivity of snow cover
684 duration in Austria, International Journal of Climatology, 20, 615-640, 2000.
685 Harris, A., and Dash, J.: The potential of the MERIS Terrestrial Chlorophyll Index for
686 carbon flux estimation, Remote Sens. Environ., 114, 1856-1862,
687 10.1016/j.rse.2010.03.010, 2010.
688 Hmimina, G., Dufrene, E., Pontailler, J. Y., Delpierre, N., Aubinet, M., Caquet, B., de
689 Grandcourt, A., Burban, B., Flechard, C., Granier, A., Gross, P., Heinesch, B.,
690 Longdoz, B., Moureaux, C., Ourcival, J. M., Rambal, S., Saint Andre, L., and
691 Soudani, K.: Evaluation of the potential of MODIS satellite data to predict
692 vegetation phenology in different biomes: An investigation using ground-based
693 NDVI measurements, Remote Sens. Environ., 132, 145-158,
694 10.1016/j.rse.2013.01.010, 2013.
695 Huete, A., Didan, K., Miura, T., Rodriguez, E. P., Gao, X., and Ferreira, L. G.:
696 Overview of the radiometric and biophysical performance of the MODIS vegetation
697 indices, Remote Sens. Environ., 83, 195-213, 10.1016/s0034-4257(02)00096-2,
698 2002.
699 Inouye, D. W.: The ecological and evolutionary significance of frost in the context of
700 climate change, Ecol. Lett., 3, 457-463, 2000.
701 Jeong, S. J., Ho, C. H., Gim, H. J., and Brown, M. E.: Phenology shifts at start vs. end
702 of growing season in temperate vegetation over the Northern Hemisphere for the
703 period 1982-2008, Global Change Biol., 17, 2385-2399, 10.1111/j.1365-
704 2486.2011.02397.x, 2011.

705 Jia, G. S. J., Epstein, H. E., and Walker, D. A.: Greening of arctic Alaska, 1981-2001,
706 Geophys. Res. Lett., 30, 2067
707 10.1029/2003gl018268, 2003.
708 Jolly, W. M.: Divergent vegetation growth responses to the 2003 heat wave in the
709 Swiss Alps, Geophys. Res. Lett., 32, 10.1029/2005gl023252, 2005.
710 Jolly, W. M., Dobbertin, M., Zimmermann, N. E., and Reichstein, M.: Divergent
711 vegetation growth responses to the 2003 heat wave in the Swiss Alps, Geophys. Res.
712 Lett., 32, NIL_1-NIL_4, 2005.
713 Jonas, T., Rixen, C., Sturm, M., and Stoeckli, V.: How alpine plant growth is linked to
714 snow cover and climate variability, Journal of Geophysical Research-
715 Biogeosciences, 113, G03013 10.1029/2007jg000680, 2008.
716 Julitta, T., Cremonese, E., Migliavacca, M., Colombo, R., Galvagno, M., Siniscalco,
717 C., Rossini, M., Fava, F., Cogliati, S., di Cella, U. M., and Menzel, A.: Using digital
718 camera images to analyse snowmelt and phenology of a subalpine grassland, Agric.
719 For. Meteorol., 198, 116-125, 10.1016/j.agrformet.2014.08.007, 2014.
720 Kato, T., Tang, Y., Gu, S., Hirota, M., Du, M., Li, Y., and Zhao, X.: Temperature and
721 biomass influences on interannual changes in CO2 exchange in an alpine meadow
722 on the Qinghai-Tibetan Plateau, Global Change Biol., 12, 1285-1298,
723 10.1111/j.1365-2486.2006.01153.x, 2006.
724 Keller, F., Goyette, S., and Beniston, M.: Sensitivity analysis of snow cover to climate
725 change scenarios and their impact on plant habitats in alpine terrain, Clim. Change,
726 72, 299-319, 2005.
727 Körner, C.: The nutritional status of plants from high altitudes, Oecologia, 81, 623-
728 632, 1989.

729 Körner, C., Diemer, M., Sch,,ppi, B., Niklaus, P., and Arnone, I., J.: The responses of
730 alpine grassland to four seasons of CO_2enrichment: a synthesis, Acta Oecol., 18,
731 436-443, 1997.
732 Körner, C.: Alpine Plant Life, Springer Verlag, Berlin, 338 pp., 1999.
733 Kreyling, J., Beierkuhnlein, C., Pritsch, K., Schloter, M., and Jentsch, A.: Recurrent
734 soil freeze-thaw cycles enhance grassland productivity, New Phytol., 177, 938-945,
735 10.1111/j.1469-8137.2007.02309.x, 2008.
736 Kudo, G., Nordenhall, U., and Molau, U.: Effects of snowmelt timing on leaf traits,
737 leaf production, and shoot growth of alpine plants: Comparisons along a snowmelt
738 gradient in northern Sweden, Ecoscience, 6, 439-450, 1999.
739 Li, Z. Q., Yu, G. R., Xiao, X. M., Li, Y. N., Zhao, X. Q., Ren, C. Y., Zhang, L. M.,
740 and Fu, Y. L.: Modeling gross primary production of alpine ecosystems in the
741 Tibetan Plateau using MODIS images and climate data, Remote Sens. Environ., 107,
742 510-519, 10.1016/j.rse.2006.10.003, 2007.
743 Monteith, J. L.: Climate and efficiency of crop production in Britain, Philosophical
744 Transactions of the Royal Society of London Series B-Biological Sciences, 281,
745 277-294, 1977.
746 Myneni, R. B., and Williams, D. L.: ON THE RELATIONSHIP BETWEEN FAPAR
747 AND NDVI, Remote Sens. Environ., 49, 200-211, 10.1016/0034-4257(94)90016-7,
748 1994.
749 Myneni, R. B., Keeling, C. D., Tucker, C. J., Asrar, G., and Nemani, R. R.: Increased
750 plant growth in the northern high latitudes from 1981 to 1991, Nature, 386, 698-702,
751 1997.

752 Pettorelli, N., Vik, J. O., Mysterud, A., Gaillard, J. M., Tucker, C. J., and Stenseth, N.
753 C.: Using the satellite-derived NDVI to assess ecological responses to environmental
754 change, Trends Ecol. Evol., 20, 503-510, 2005.
755 Rammig, A., Jonas, T., Zimmermann, N. E., and Rixen, C.: Changes in alpine plant
756 growth under future climate conditions, Biogeosciences, 7, 2013-2024, 10.5194/bg-
757 7-2013-2010, 2010.
758 Reichstein, M., Ciais, P., Papale, D., Valentini, R., Running, S., Viovy, N., Cramer,
759 W., Granier, A., Ogee, J., Allard, V., Aubinet, M., Bernhofer, C., Buchmann, N.,
760 Carrara, A., Grunwald, T., Heimann, M., Heinesch, B., Knohl, A., Kutsch, W.,
761 Loustau, D., Manca, G., Matteucci, G., Miglietta, F., Ourcival, J. M., Pilegaard, K.,
762 Pumpanen, J., Rambal, S., Schaphoff, S., Seufert, G., Soussana, J. F., Sanz, M. J.,
763 Vesala, T., and Zhao, M.: Reduction of ecosystem productivity and respiration
764 during the European summer 2003 climate anomaly: a joint flux tower, remote
765 sensing and modelling analysis, Global Change Biol., 13, 634-651, 2007.
766 Rosseel, Y.: lavaan: An R Package for Structural Equation Modeling, Journal of
767 Statistical Software, 48, 1-36, 2012.
768 Rossini, M., Cogliati, S., Meroni, M., Migliavacca, M., Galvagno, M., Busetto, L.,
769 Cremonese, E., Julitta, T., Siniscalco, C., di Cella, U. M., and Colombo, R.: Remote
770 sensing-based estimation of gross primary production in a subalpine grassland,
771 Biogeosciences, 9, 2565-2584, 10.5194/bg-9-2565-2012, 2012.
772 Salomonson, V. V., and Appel, I.: Estimating fractional snow cover from MODIS
773 using the normalized difference snow index, Remote Sens. Environ., 89, 351-360,
774 10.1016/j.rse.2003.10.016, 2004.
775 Savitzky, A., and Golay, M. J. E.: Smoothing and Differentiation of Data by
776 Simplified Least Squares Procedures, Analytical Chemistry, 36, 1627-1639, 1964.

777 Stockli, R., and Vidale, P. L.: European plant phenology and climate as seen in a 20-
778 year AVHRR land-surface parameter dataset, Int. J. Remote Sens., 25, 3303-3330,
779 2004.
780 Studer, S., Stockli, R., Appenzeller, C., and Vidale, P. L.: A comparative study of
781 satellite and ground-based phenology, International Journal of Biometeorology, 51,
782 405-414, 10.1007/s00484-006-0080-5, 2007.
783 Tan, B., Woodcock, C. E., Hu, J., Zhang, P., Ozdogan, M., Huang, D., Yang, W.,
784 Knyazikhin, Y., and Myneni, R. B.: The impact of gridding artifacts on the local
785 spatial properties of MODIS data: Implications for validation, compositing, and
786 band-to-band registration across resolutions, Remote Sens. Environ., 105, 98-114,
787 10.1016/j.rse.2006.06.008, 2006.
788 Ustin, S. L., Roberts, D. A., Gamon, J. A., Asner, G. P., and Green, R. O.: Using
789 imaging spectroscopy to study ecosystem processes and properties, Bioscience, 54,
790 523-534, 2004.
791 Vittoz, P., Randin, C., Dutoit, A., Bonnet, F., and Hegg, O.: Low impact of climate
792 change on subalpine grasslands in the Swiss Northern Alps, Global Change Biol.,
793 15, 209-220, 10.1111/j.1365-2486.2008.01707.x, 2009.
794 Walker, M. D., Webber, P. J., Arnold, E. H., and Ebert-May, D.: Effects of
795 interannual climate variation on aboveground phytomass in alpine vegetation,
796 Ecology, 75, 490-502, 1994.
797 Wipf, S., and Rixen, C.: A review of snow manipulation experiments in Arctic and
798 alpine tundra ecosystems, Polar Res., 29, 95-109, 10.1111/j.1751-
799 8369.2010.00153.x, 2010.
800 Yuan, W. P., Cai, W. W., Liu, S. G., Dong, W. J., Chen, J. Q., Arain, M. A., Blanken,
801 P. D., Cescatti, A., Wohlfahrt, G., Georgiadis, T., Genesio, L., Gianelle, D., Grelle,

802 A., Kiely, G., Knohl, A., Liu, D., Marek, M. V., Merbold, L., Montagnani, L.,
803 Panferov, O., Peltoniemi, M., Rambal, S., Raschi, A., Varlagin, A., and Xia, J. Z.:
804 Vegetation-specific model parameters are not required for estimating gross primary
805 production, Ecol. Model., 292, 1-10, 10.1016/j.ecolmodel.2014.08.017, 2014.
806 Zinger, L., Shahnavaz, B., Baptist, F., Geremia, R. A., and Choler, P.: Microbial
807 diversity in alpine tundra soils correlates with snow cover dynamics, Isme Journal,
808 3, 850-859, 10.1038/ismej.2009.20, 2009.
809
810

Figure caption

Figure 1. (A) Location map of the 121 polygons across the seventeen climatologically defined massifs of the French Alps. (B) Number of polygons per massif.

Figure 2. Yearly course of NDVI and NDSI showing the different variables used in this study: date of snowmelt (TSNOWmelt), maximum NDVI (NDVImax) and date of NDVImax (TNDVImax), date of snowfall (TSNOWfall), length of the snow-free period (Psf), length of the initial growth period (Pg), length of the senescence period (Ps), and time-integrated NDVI over the growth period (NDVIintg) and over the senescence period (NDVIints).

Figure 3. Frequency distribution of the relative contribution of Pg and Ps to Psf (A), of NDVIintg and NDVIints to NDVIint (B) and of GPPintg and GPPints to GPPint (C). Values were calculated for each year and for each polygon.

Figure 4. Inter-annual standardized anomalies for NDVImax (A), Psf (B), NDVIint (C) and GPPint (D).

Figure 5. Path analysis diagram showing the interacting effects of meteorological forcing, snow cover duration and NDVImax on NDVIint (A, B) and GPPint (C, D). For each proxy of productivity, separate models for the period of growth (A, C) and the period of senescence (B, D) are shown. Line thickness of arrows is proportional to standardized path coefficients which are indicated on the right or above each arrow.

836 Values in italics indicate paths that can be removed without penalizing model AIC
837 (see Table 2). Solid line (or dotted lines) indicates a significant positive (or negative)
838 effect at $P<0.05$. Double lined arrows correspond to fixed parameters. Abbreviations
839 include TEMP, averaged daily mean temperature (or senescence period); PREC
840 averaged daily sum of precipitation; FrEv: number of frost events. Letter g (or s) is for
841 the initial growth period (or the senescence period). Spring means the months of
842 March and April. Fall means the months of October and November.
843
844 **Figure S1**. Ground-based observations of TSNOWmelt and TSNOWfall at Lautaret
845 pass from 2012 onwards (dotted lines) superimposed on the NDVI and NDSI time
846 series obtained from MODIS (8-days composite). The comparison is made for a single
847 500m MOD09A1 pixel that corresponds to a relatively flat area dominated by
848 subalpine grasslands at a mean elevation of 2000 m.
849
850 **Figure S2**. Sensitivity of the length of the snow free period (Psf) to changes in the
851 NDVI/NDSI thresholds. Psf changes are simulated for four thresholds and for the
852 1820 polygon x year combinations. Numbers above each boxplot indicate the
853 percentage of combinations exhibiting a shortening of Psf larger than two days (when
854 the threshold is increased) and a lengthening of Psf larger than three days (when the
855 threshold is decreased).
856
857 **Figure S3**. (A) Relationships between the inter-annual variations (standard deviation)
858 of EVIint and NDVIint. One point corresponds to one polygon. (B) Frequency
859 distribution of the relative contribution of EVIintg and EVIints to EVIint (to be
860 compared to Fig. 3C). Values were calculated for each year and for each polygon.

861

862 **Figure S4**. Relationships between TSNOWmelt and TNDVImax (A) or NDVImax

863 (B). Points correspond to every year x polygon combination. The dash-dotted line in

864 (A) indicates a 1:1 relationship. Dotted lines show average values for each variable.

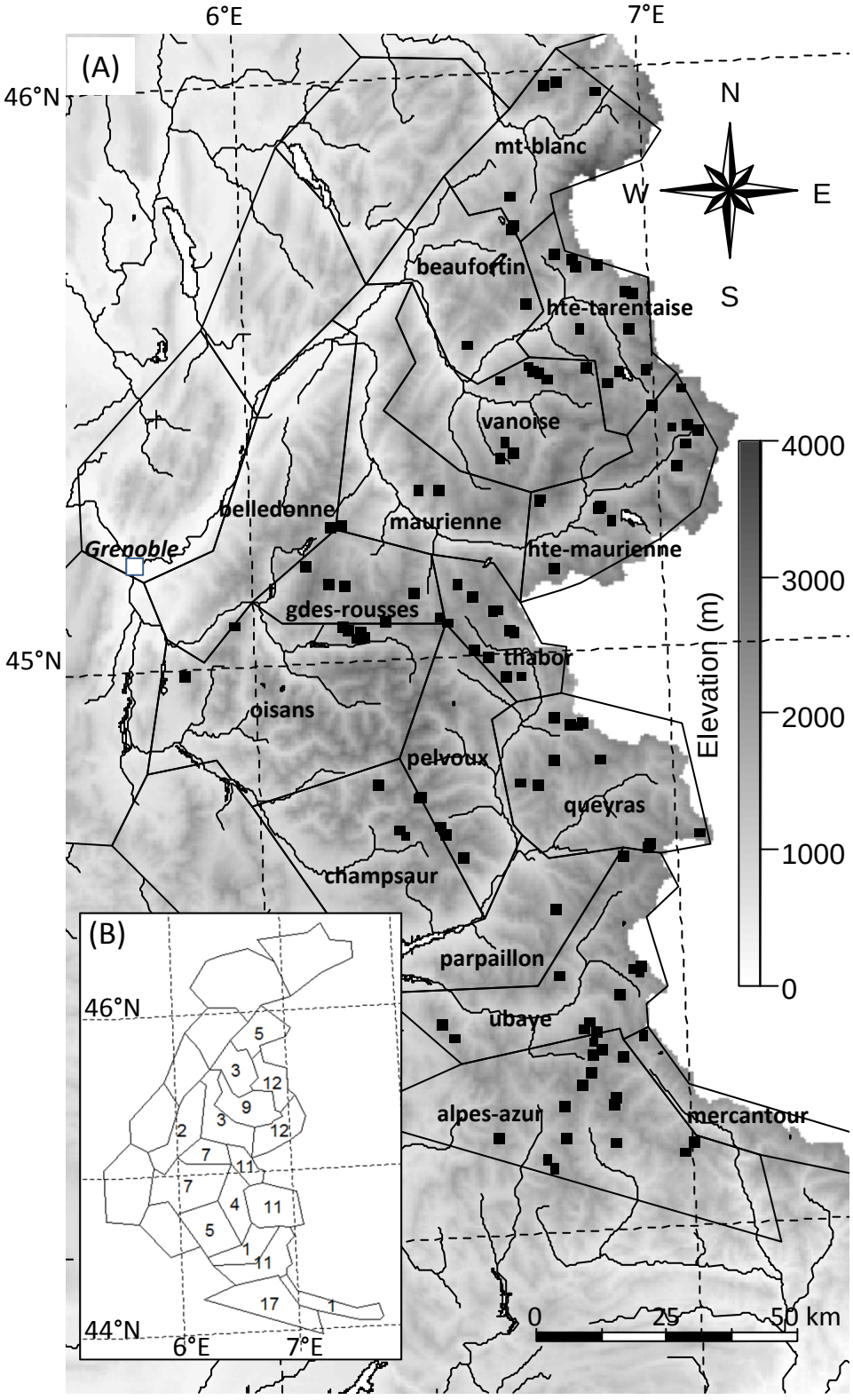
(A)
6°E
7°E
46°N
45°N
N
W
E
S
mt-blanc
beaufortin
hte-tarentaise
vanoise
belledonne
maurienne
hte-maurienne
Grenoble
gdes-rousses
thabor
oisans
pelvoux
queyras
champsaur
parpaillon
ubaye
alpes-azur
mercantour
Elevation (m)
4000
3000
2000
1000
0
0
25
50 km
(B)
46°N
44°N
6°E
7°E
5
3
12
9
3
12
2
7
11
7
4
11
5
1
11
17
1

Figure 1

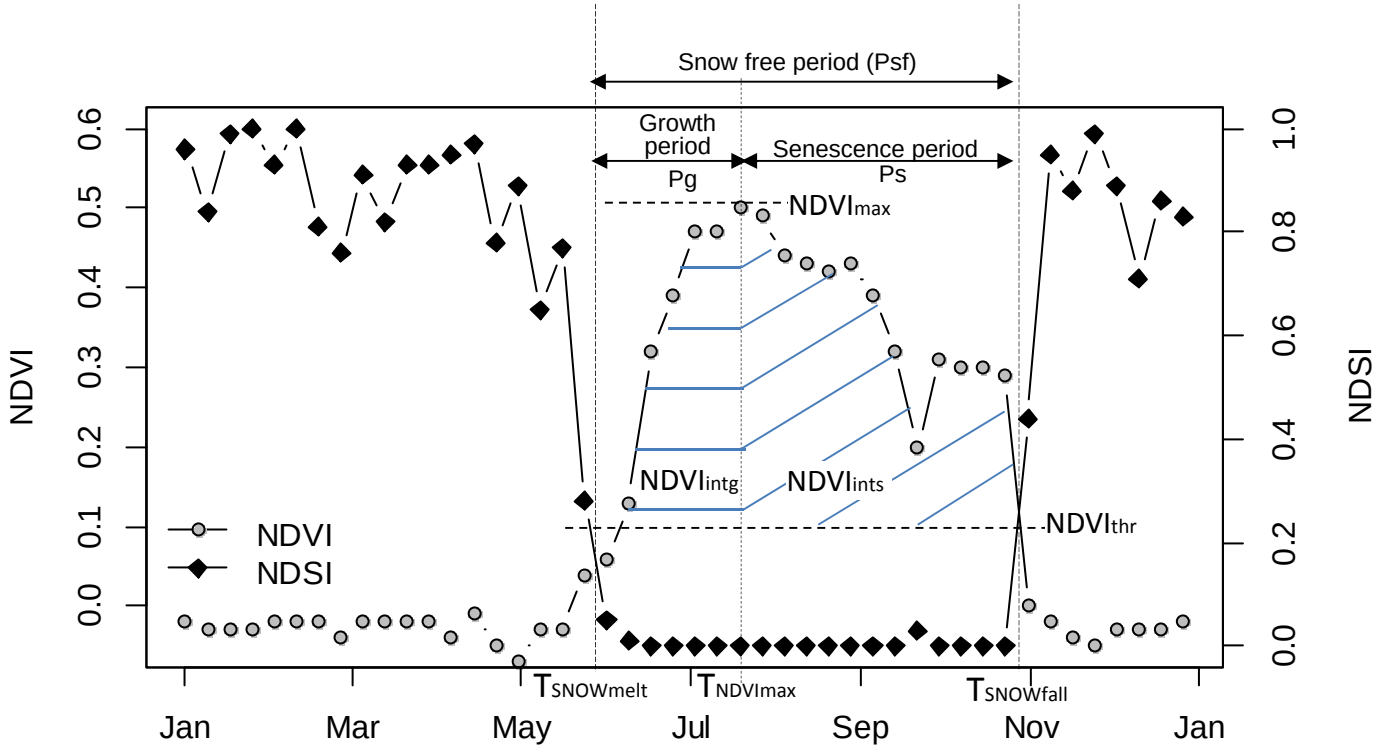
Snow free period (Psf)
Growth period
Pg
Senescence period
Ps
NDVImax
NDVIintg
NDVIints
NDVIthr
NDVI
NDSI
TSNOWmelt
TNDVImax
TSNOWfall
Jan
Mar
May
Jul
Sep
Nov
Jan
0.0
0.1
0.2
0.3
0.4
0.5
0.6
0.0
0.2
0.4
0.6
0.8
1.0

Figure 2

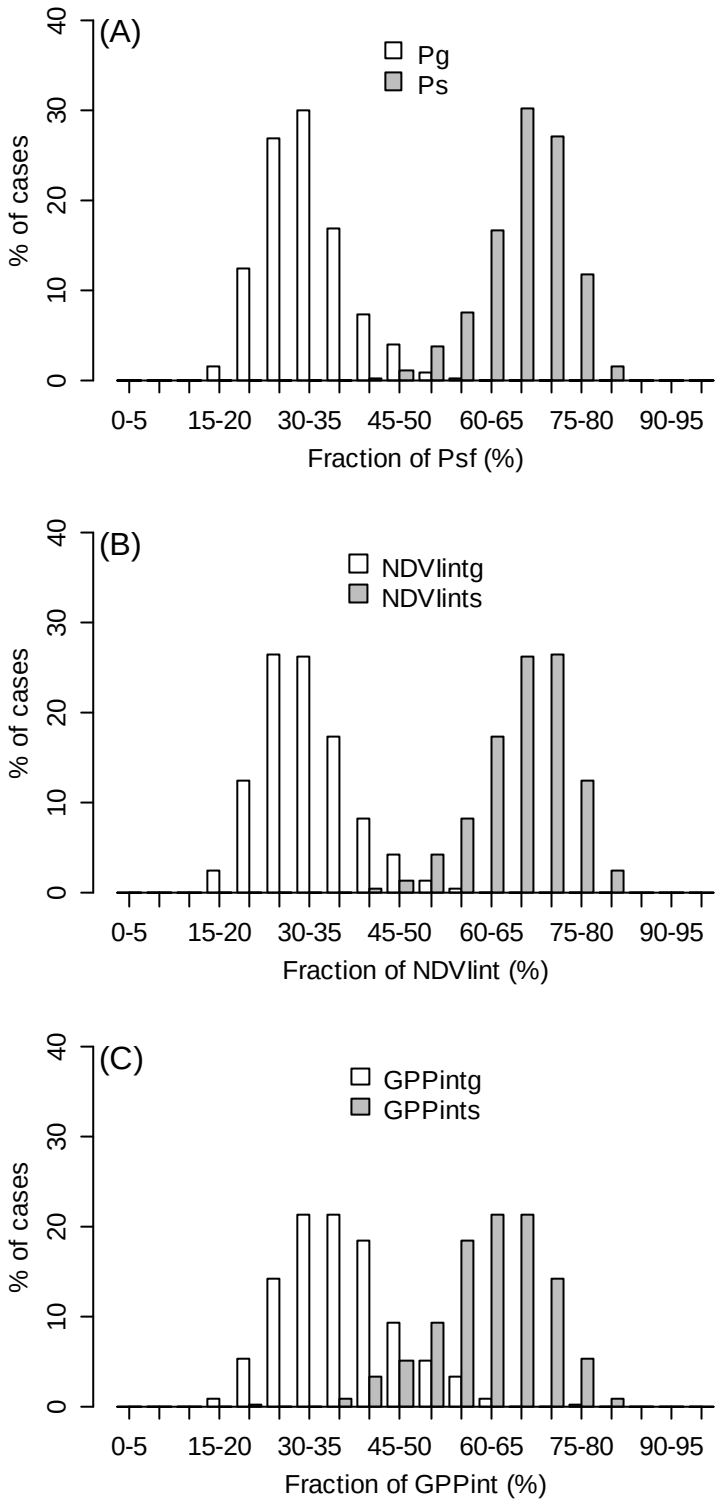
(A)
Pg
Ps
% of cases
0
10
20
30
40
0-5
15-20
30-35
45-50
60-65
75-80
90-95
Fraction of Psf (%)
(B)
NDVIintg
NDVIints
% of cases
0
10
20
30
40
0-5
15-20
30-35
45-50
60-65
75-80
90-95
Fraction of NDVIint (%)
(C)
GPPintg
GPPints
% of cases
0
10
20
30
40
0-5
15-20
30-35
45-50
60-65
75-80
90-95
Fraction of GPPint (%)

Figure 3

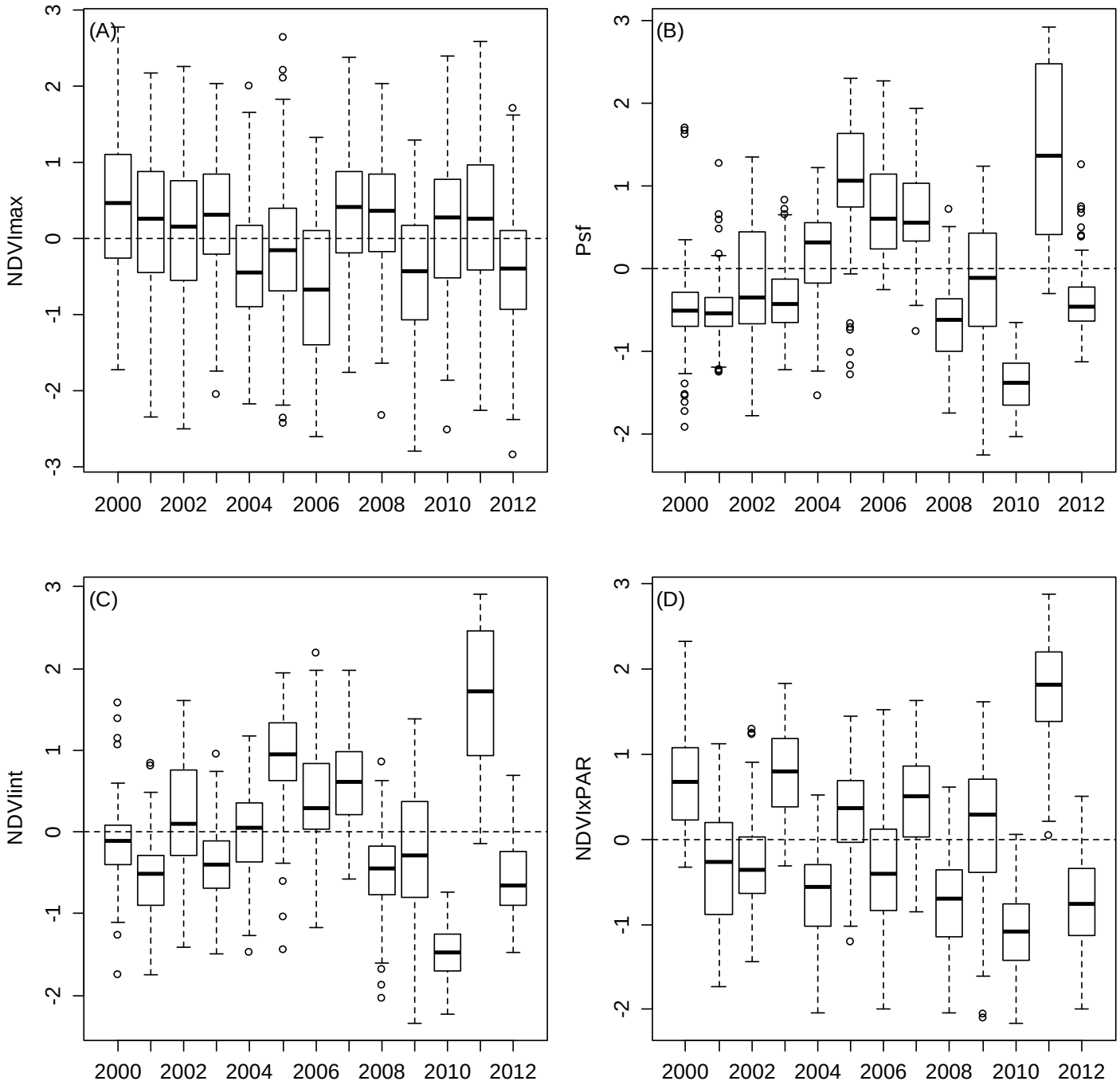
(A)
NDVImax
(B)
Psf
(C)
NDVIint
(D)
NDVIxPAR
2000
2002
2004
2006
2008
2010
2012

Figure 4

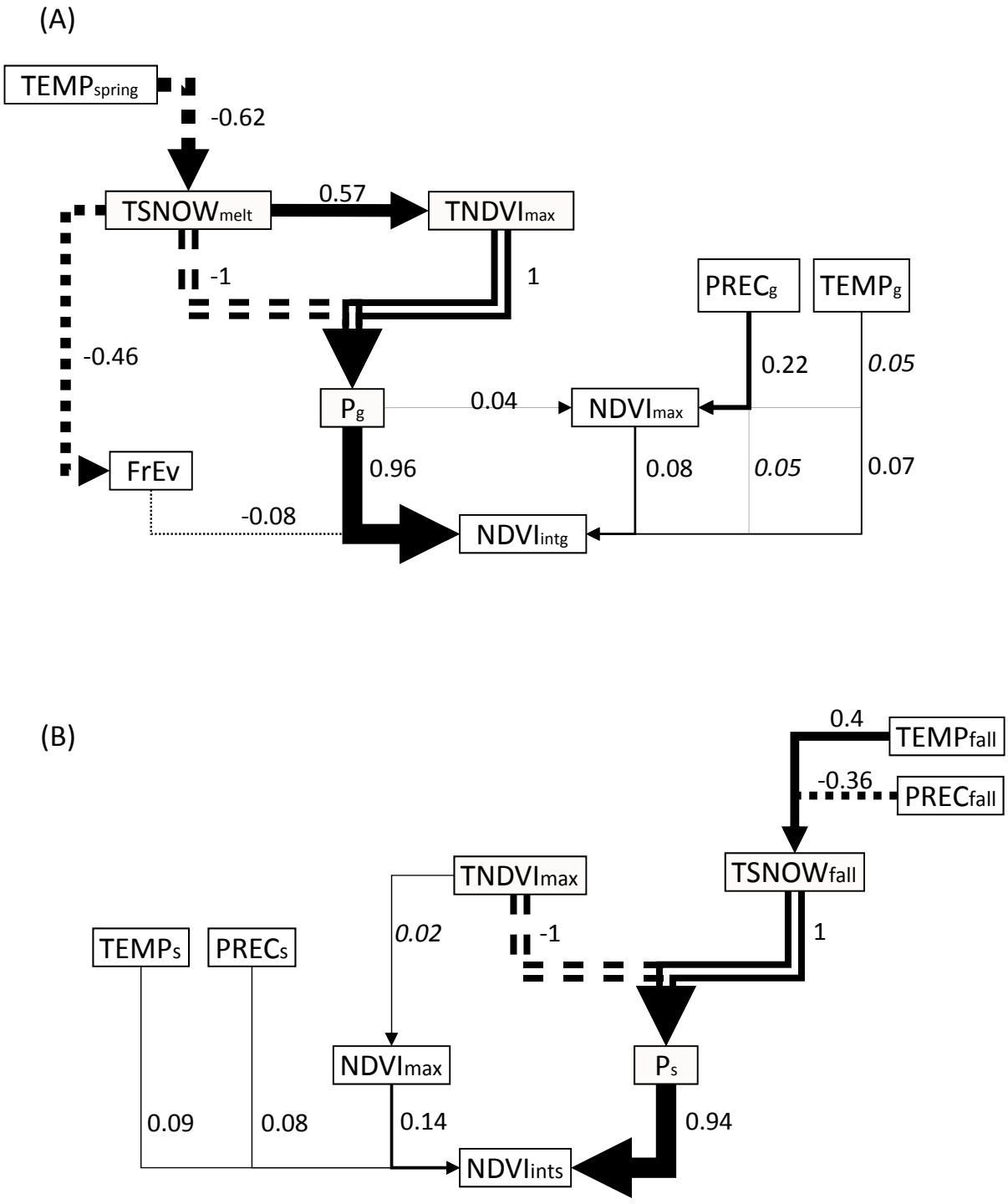
(A)
TEMPspring
-0.62
TSNOWmelt
0.57
TNDVImax
-1
1
PRECg
TEMPg
-0.46
0.22
0.05
Pg
0.04
NDVImax
FrEv
0.96
0.08
0.05
0.07
-0.08
NDVIintg
(B)
0.4
TEMPfall
-0.36
PRECfall
TNDVImax
TSNOWfall
TEMPs
PRECs
0.02
-1
1
NDVImax
Ps
0.09
0.08
0.14
0.94
NDVIints

Figure 5

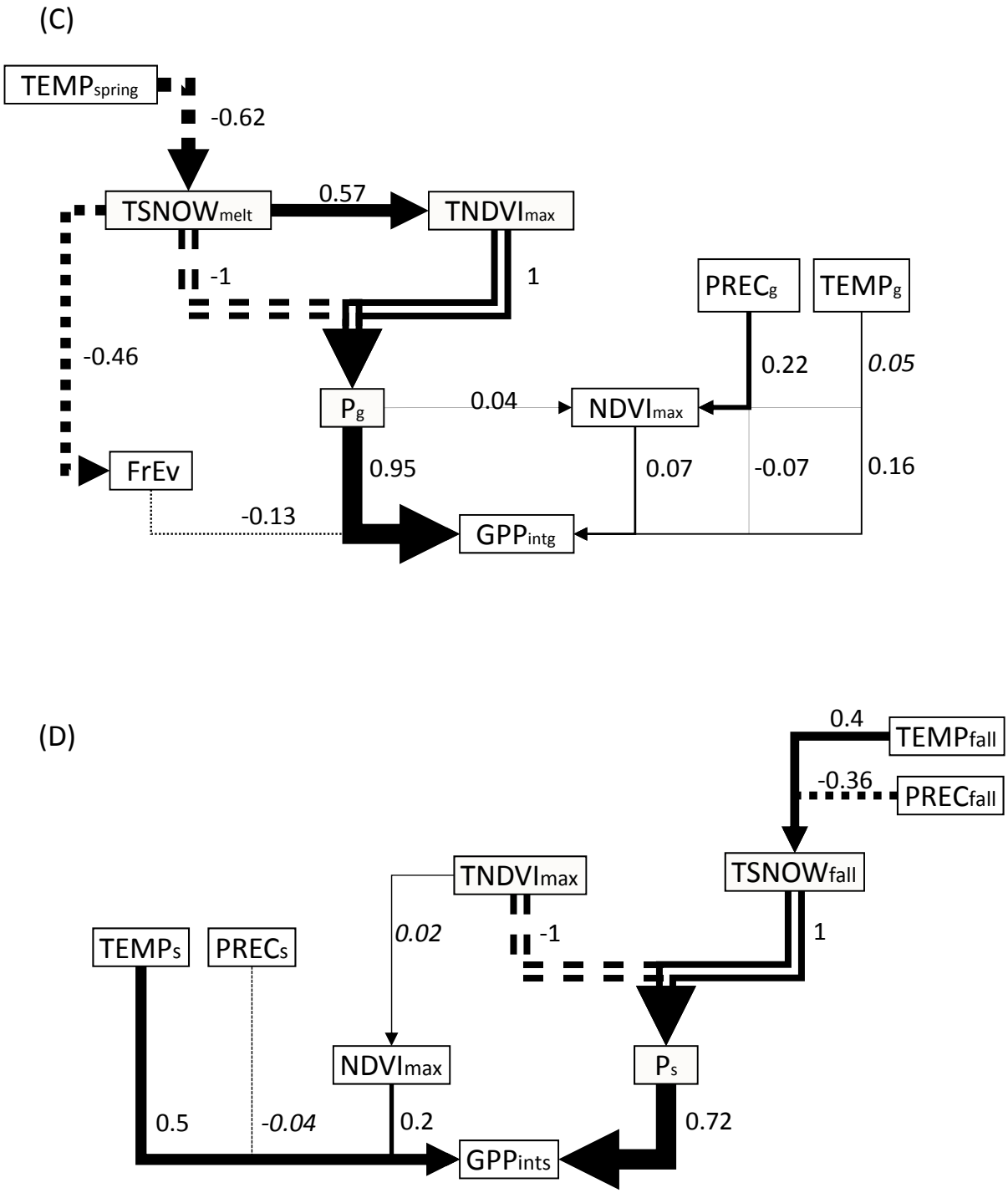

Figure 5 (continued)

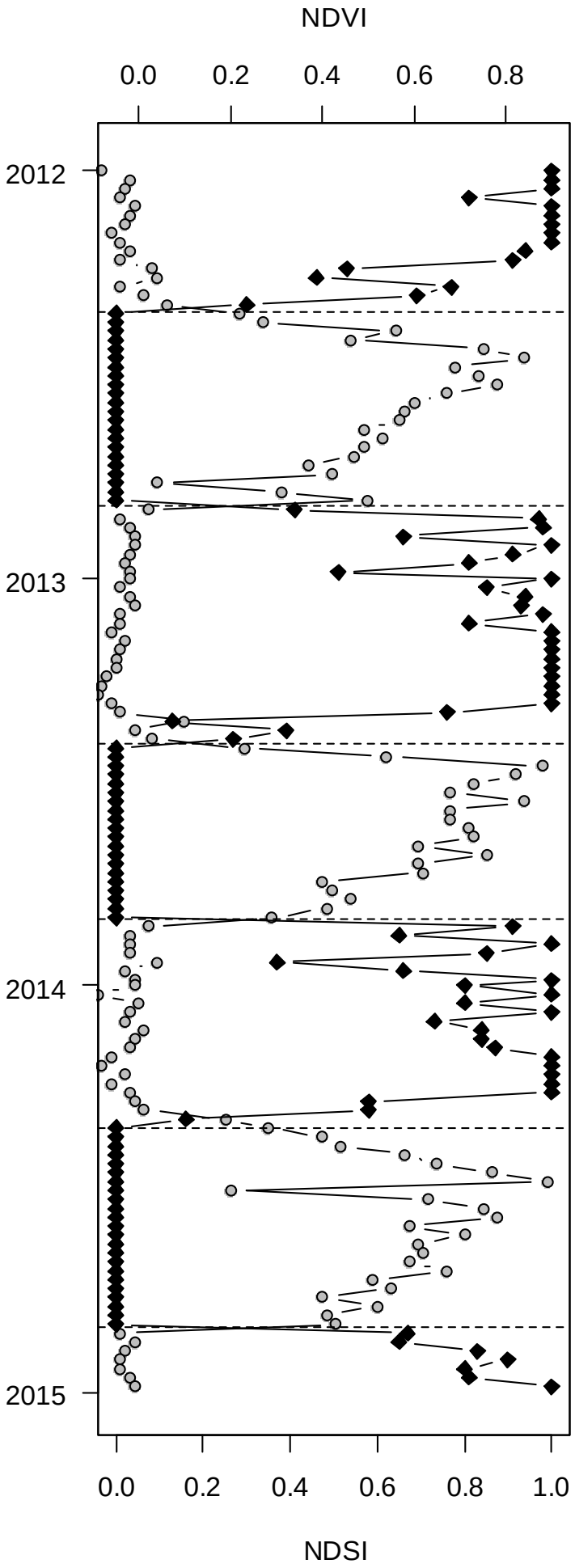

Figure S1

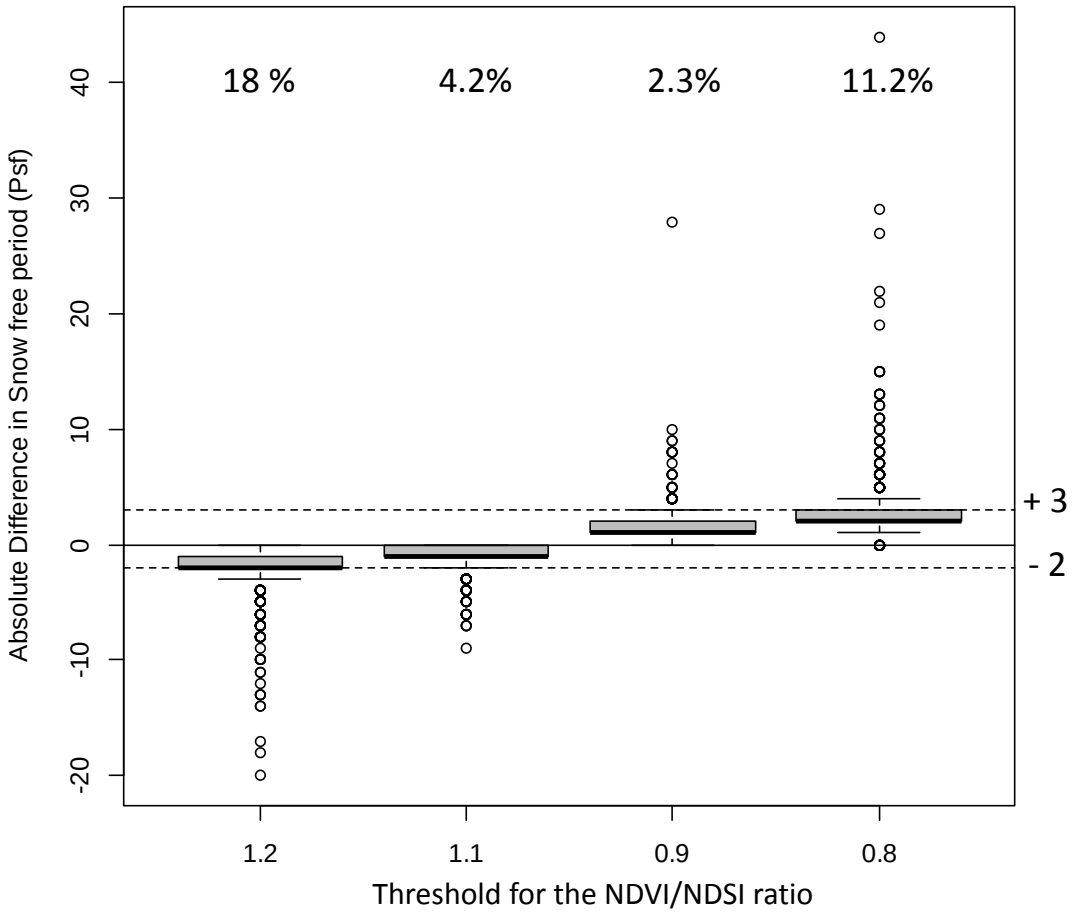
18 %
4.2%
2.3%
11.2%
+ 3
- 2
Absolute Difference in Snow free period (Psf)
40
30
20
10
0
-10
-20
1.2
1.1
0.9
0.8
Threshold for the NDVI/NDSI ratio

Figure S2

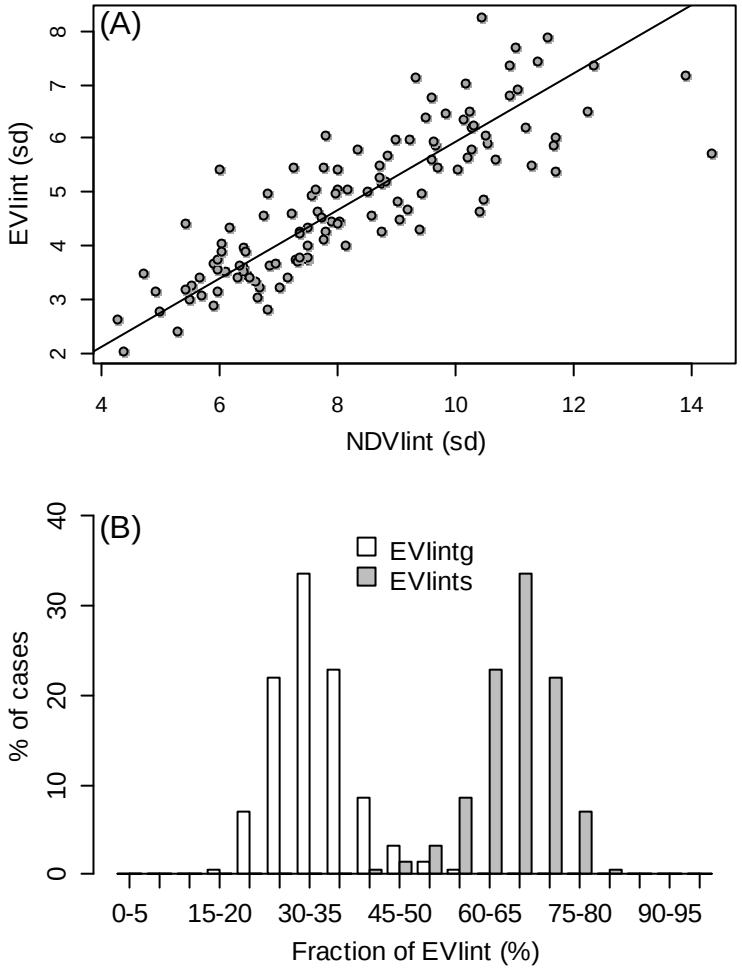
(A)
EVIint (sd)
NDVIint (sd)
2
3
4
5
6
7
8
4
6
8
10
12
14
(B)
EVIintg
EVIints
% of cases
0
10
20
30
40
0-5
15-20
30-35
45-50
60-65
75-80
90-95
Fraction of EVIint (%)

Figure S3

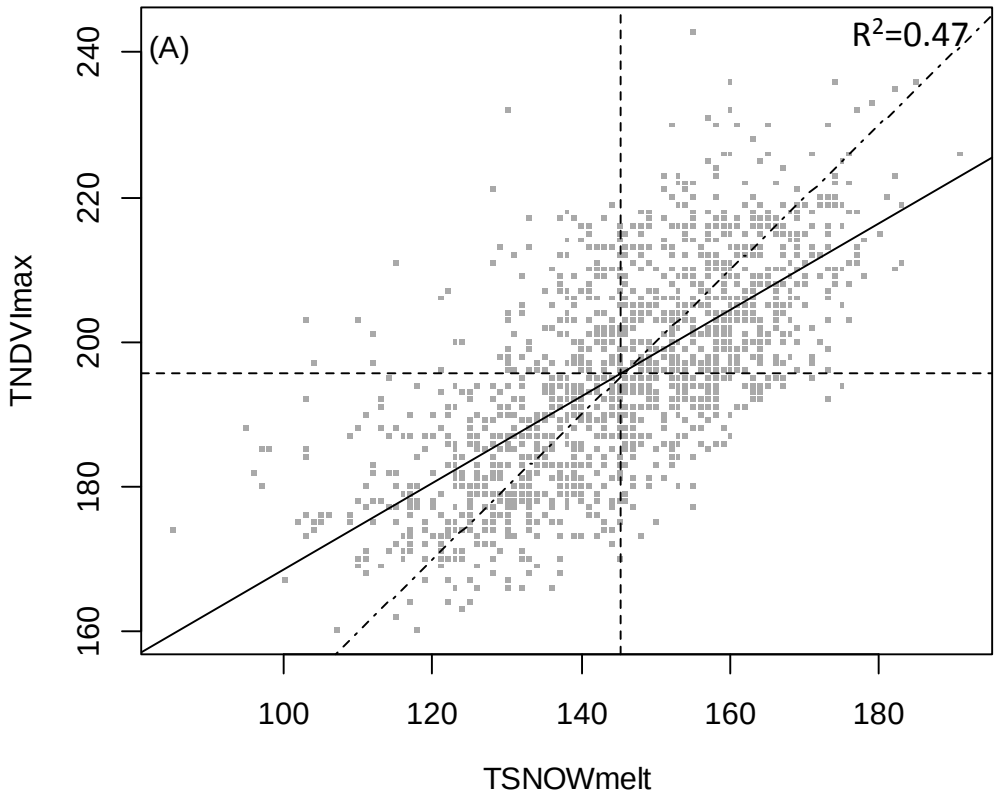
(A)
R^2=0.47
TNDVImax
240
220
200
180
160
100
120
140
160
180
TSNOWmelt

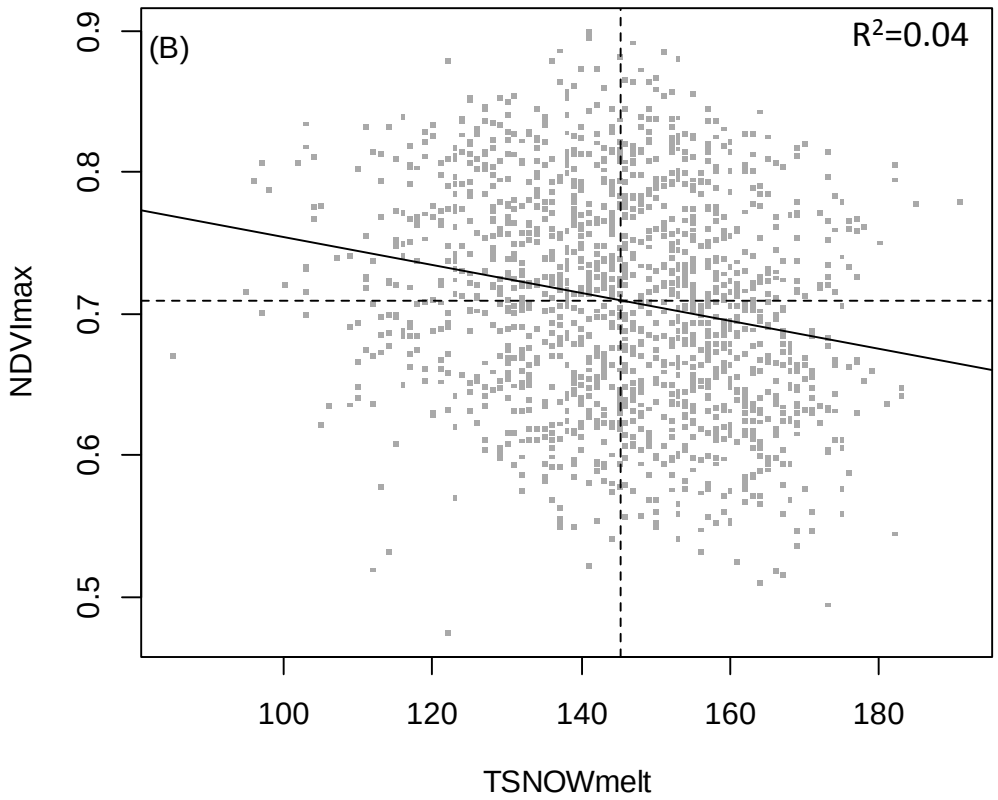
(B)
R^2=0.04
NDVImax
0.9
0.8
0.7
0.6
0.5
100
120
140
160
180
TSNOWmelt

Figure S4